Channel Estimation in RIS-Aided Communications With Interference

Wen-Xuan Long, *Graduate Student Member, IEEE*, Marco Moretti, *Member, IEEE*, Luca Sanguinetti, *Senior Member, IEEE*, and Rui Chen, *Member, IEEE*

***Abstract*—This letter considers the channel estimation problem when a reconfigurable intelligent surface (RIS) is used to aid wireless communications between a base station (BS) and an user equipment (UE). Unlike prior works, we assume that the directional or isotropic interference from other UEs is present at the location where the RIS is located. To address the problem, we make use of a two-stage training phase that, for any RIS configuration, operates as follows. In the first phase, the UE is not transmitting and the BS estimates the interference contribution that reaches it. This is then subtracted in the second phase during which the cascaded channel from the UE to the BS through each RIS element is estimated. In doing so, no a priori knowledge of the spatial correlation matrices of the interference and cascaded channels is assumed. The mean-square-error of channel estimates is computed and used to optimize the phase-shift configurations of RIS elements. Numerical results prove the effectiveness of the proposed approach in directional or isotropic channel and interference scenarios.**

***Index Terms*—Reconfigurable intelligent surface (RIS), mean square error (MSE), channel estimation.**

I. Introduction

THE DEPLOYMENT of reconfigurable intelligent surfaces (RIS) in next-generation wireless communications holds great promise [1], [2]. RIS technology allows for partial control of the radio environment, utilizing planar arrays composed of numerous low-cost passive reflecting elements. By adjusting the impedance of these elements, the RIS can intelligently induce controllable phase-shifts in incoming signals, redirecting them towards the desired receiver [3]. It's important to note that RIS does not amplify signals, but rather relies on intelligent reflection. To ensure a satisfactory signal-to-noise ratio (SNR) at the receiver, a significant surface area is required. Consequently, as the size of the RIS grows larger, it becomes more susceptible to interference [4].

Manuscript received 21 April 2023; revised 10 June 2023; accepted 27 June 2023. Date of publication 3 July 2023; date of current version 9 October 2023. The work of Wen-Xuan Long and Rui Chen was supported by the National Natural Science Foundation of China under Grant 62271376. The work of Marco Moretti and Luca Sanguinetti was supported in part by the Italian Ministry of Education and Research (MUR) in the Framework of the FoReLab Project (Departments of Excellence) and in part by the University of Pisa under Project PRA-2022-2023-91. The associate editor coordinating the review of this article and approving it for publication was M. Kishk. *(Corresponding author: Wen-Xuan Long.)*

Wen-Xuan Long is with the State Key Laboratory of Integrated Service Networks, Xidian University, Xi'an 710071, Shaanxi, China, and also with the Dipartimento di Ingegneria dell'Informazione, University of Pisa, 56122 Pisa, Italy (e-mail: wxlong@stu.xidian.edu.cn).

Marco Moretti and Luca Sanguinetti are with the Dipartimento di Ingegneria dell'Informazione, University of Pisa, 56122 Pisa, Italy (e-mail: marco.moretti@iet.unipi.it; luca.sanguinetti@unipi.it).

Rui Chen is with the State Key Laboratory of Integrated Service Networks, Xidian University, Xi'an 710071, Shaanxi, China (e-mail: rchen@xidian.edu.cn).

Digital Object Identifier 10.1109/LWC.2023.3291500

In order to enhance the channel gain of a system assisted by RIS in the presence of interference, it is crucial to appropriately configure the phase shifts of the RIS elements to shape the reflected wavefront [5]. This necessitates accurate estimation of the cascaded channel, which comprises the path from the user equipment (UE) to the base station (BS) reflected by the RIS elements. While the channel estimation of RIS-aided wireless communication has been extensively investigated [6], [7], [8], [9], existing research has *not* taken into account the impact of existing interference on the channel estimation process for RIS-aided systems.

In this letter, we present a channel estimation scheme for a wireless communication system aided by RIS in the presence of directional or isotropic interference. The proposed scheme divides the estimation process into two stages. The first stage focuses on estimating the interference, while the second stage estimates the cascaded channel. To ensure a low system complexity and minimize the required number of pilot symbols, we draw inspiration from recent work [9] and employ the *conservative* reduced-subspace least squares (RS-LS) estimator in both stages. This choice allows us to achieve precise estimation of the directional/isotropic cascaded channel without relying on any interference- or channel-related a priori knowledge. Additionally, we optimize the pilot length and phase-shift configurations of the RIS elements to minimize the mean-square error (MSE) of the cascaded channel estimation. In typical directional/isotropic channel and interference scenarios, our proposed conservative RS-LS-based estimation scheme outperforms conventional schemes that do not estimate the interference. Moreover, it can be implemented with lower pilot overhead requirements.

II. System Model

Consider a system in which a single-antenna UE communicates to a BS with the aid of a RIS. The BS antennas are deployed as a uniform planar array (UPA) with M_H and M_V number of elements per row and per column, and we have $M = M_H M_V$ antennas in total. The RIS is composed of N passive reconfigurable elements that form a UPA with N_H rows and N_V columns, where $N = N_H N_V$. Each RIS element introduces a controllable phase-shift $\phi_n \in [0, 2\pi)$ for directional reflection of incoming signals. We assume a time-varying narrowband channel and employ the conventional block fading model, in which the time/frequency resources are divided into independent coherence blocks.

We call $\mathbf{h} \in \mathbb{C}^N$ the channel vector between the RIS and UE and model it as $\mathbf{h} \sim \mathcal{N}_{\mathbb{C}}(\mathbf{0}_N, \mathbf{R}_h)$, where $\mathbf{R}_h$ is the spatial correlation matrix. The latter can be computed as [10], [11]

$$\mathbf{R}_h = \beta_h \int \int_{-\pi/2}^{\pi/2} f_h(\varphi, \theta) \mathbf{a}(\varphi, \theta) \mathbf{a}^{\mathrm{H}}(\varphi, \theta) d\theta d\varphi, \quad (1)$$

where β_h is the channel gain, φ and θ are the azimuth and elevation angles, $f_h(\varphi,\theta)$ and $\mathbf{a}(\varphi,\theta)$ are the normalized spatial scattering function and the array response vector, respectively.

In an isotropic scattering environment, $\mathbf{R}_h$ reduces to $\mathbf{R}_h = \beta_h \mathbf{R}_{\text{iso}}$ with [10]

$$[\mathbf{R}_{\text{iso}}]_{n,k} = \text{sinc}\left(2\sqrt{(d_H^{n,k})^2 + (d_V^{n,k})^2}/\lambda\right), \tag{2}$$

where $\text{sinc}(\cdot)$ is the sinc function, $d_H^{n,k}$ and $d_V^{n,k}$ are the horizontal and vertical distances between elements n and k, respectively.

We denote $g_{m,n} \in \mathbb{C}$ the channel from RIS element n to BS element m. Then, we define $\mathbf{g}_m = [g_{m,1}, g_{m,2}, \ldots, g_{m,N}]^{\text{T}} \in \mathbb{C}^N$ from the RIS to BS element m. Similarly, $\mathbf{g}'_n = [g_{1,n}, g_{2,n}, \ldots, g_{M,n}]^{\text{T}} \in \mathbb{C}^M$ is the channel vector from RIS element n to BS array. They are distributed as $\mathbf{g}_m \sim \mathcal{N}_{\mathbb{C}}(\mathbf{0}_N, [\mathbf{R}_{g'}]_{m,m}\mathbf{R}_g)$ and $\mathbf{g}'_n \sim \mathcal{N}_{\mathbb{C}}(\mathbf{0}_M, [\mathbf{R}_g]_{n,n}\mathbf{R}_{g'})$, where $\mathbf{R}_g$ and $\mathbf{R}_{g'}$ are spatial correlation matrices of $\mathbf{g}_m$ and $\mathbf{g}'_n$. We assume that $\mathbf{g}_m$ (and thus $\mathbf{g}'_n$) and $\mathbf{h}$ are independent.

We model the interference as the vector $\mathbf{n} \sim \mathcal{N}_{\mathbb{C}}(\mathbf{0}_N, \mathbf{R}_n)$ and assume that it stays approximately constant for the entire pilot duration. This depicts several possible interference scenarios, such as the presence of slow-varying electromagnetic interference (EMI) [4] or the presence of other UEs transmitting simultaneously a pilot preamble. The spatial correlation matrix $\mathbf{R}_n$ of the interference has the same form of (1), i.e.,

$$\mathbf{R}_n = \sigma_n^2 \int \int_{-\pi/2}^{\pi/2} f_n(\varphi,\theta)\mathbf{a}(\varphi,\theta)\mathbf{a}^{\text{H}}(\varphi,\theta)\, d\theta\, d\varphi, \tag{3}$$

but with a different spatial scattering function $f_n(\varphi,\theta)$. If the interference is isotropic, then (3) reduces to $\mathbf{R}_n = \sigma_n^2 \mathbf{R}_{\text{iso}}$.

III. Pilot Transmission and Channel Estimation

To optimize the RIS phase-shifts and signal precoding during the data transmission phase, the BS needs to perform channel estimation. We assume that τ samples are reserved for the training phase. The direct link between the BS and UE is neglected to focus on the cascaded channel estimation.

Due to the presence of interference, we propose a two-stage training phase to address interference in the system. The first stage involves $\tau_1 \leq \tau$ samples, where the UE is inactive and the BS estimates the interference. In the second stage, utilizing $\tau_2 = \tau - \tau_1$ samples, we estimate the cascaded channel through the RIS elements after removing the interference. This approach allows for accurate channel estimation while mitigating the impact of interference.

A. First Stage: Interference Estimation

During the first stage, the UE is not transmitting, and the BS only receives the interference reflected by the RIS. Hence, the signal vector $\mathbf{y}_m^{(1)} \in \mathbb{C}^{\tau_1}$ received by antenna m at the BS can be expressed as:

$$\mathbf{y}_m^{(1)} = \mathbf{\Phi}^{(1)}(\mathbf{g}_m \odot \mathbf{n}) + \mathbf{z}_m^{(1)}, \tag{4}$$

where $\mathbf{y}_m^{(1)} = [y_{m,1}^{(1)}, y_{m,2}^{(1)}, \ldots, y_{m,\tau_1}^{(1)}]^{\text{T}}$, $\mathbf{\Phi}^{(1)} \in \mathbb{C}^{\tau_1 \times N}$ with $[\mathbf{\Phi}^{(1)}]_{i,n} = e^{-j\phi_n^i}$ is the RIS phase-shift matrix during the first stage, $\odot$ is the Hadamard product, $\mathbf{z}_m^{(1)} \sim \mathcal{N}_{\mathbb{C}}(\mathbf{0}_{\tau_1}, \sigma^2\mathbf{I}_{\tau_1})$ is the additive white Gaussian noise. Collecting all the vectors $\{\mathbf{y}_m^{(1)}; m = 1, \ldots, M\}$ into an $M\tau_1$-dimensional vector yields

$$\mathbf{y}^{(1)} = \mathbf{\Phi}_M^{(1)}\mathbf{e} + \mathbf{z}^{(1)}, \tag{5}$$

where $\mathbf{\Phi}_M^{(1)} = \mathbf{I}_M \otimes \mathbf{\Phi}^{(1)}$ and $\mathbf{e}$ is the NM-dimensional vector obtained by concatenating the vectors $\{\mathbf{g}_m \odot \mathbf{n}; m = 1, \ldots, M\}$. We denote $\mathbf{R}_e = \mathbf{R}_{g'} \otimes (\mathbf{R}_g \odot \mathbf{R}_n)$ and call $r_e = \text{rank}\{\mathbf{R}_e\}$. The eigenvalue decomposition (EVD) of $\mathbf{R}_e$ is

$$\mathbf{R}_e = \mathbf{U}_e^{\text{s}} \mathbf{\Lambda}_e (\mathbf{U}_e^{\text{s}})^{\text{H}}, \tag{6}$$

where $\mathbf{U}_e^{\text{s}} \in \mathbb{C}^{MN \times r_e}$ is the matrix collecting the eigenvectors that span the signal subspace containing the vector $\mathbf{e}$, which can thus be represented as $\mathbf{e} = \mathbf{U}_e^{\text{s}}\mathbf{a}$ [9], [11], with $\mathbf{a} \in \mathbb{C}^{r_e}$. The RS-LS estimate of $\mathbf{e}$ is obtained as

$$\hat{\mathbf{e}}_{\text{RS-LS}} = \mathbf{U}_e^{\text{s}}\, \mathbf{F}\left(\mathbf{U}_e^{\text{s}}, \mathbf{\Phi}_M^{(1)}\right)^{-1} \mathbf{U}_e^{\text{s}\,\text{H}} \mathbf{\Phi}_M^{(1)\,\text{H}} \mathbf{y}^{(1)}, \tag{7}$$

where we have defined

$$\mathbf{F}\left(\mathbf{U}_e^{\text{s}}, \mathbf{\Phi}_M^{(1)}\right) = \mathbf{U}_e^{\text{s}\,\text{H}} \mathbf{\Phi}_M^{(1)\,\text{H}} \mathbf{\Phi}_M^{(1)} \mathbf{U}_e^{\text{s}}. \tag{8}$$

B. Second Stage: Cascaded Channel Estimation

In the second stage, the UE transmits a predefined training sequence. For simplicity, we assume that it transmits $\sqrt{\rho}$ during all the τ_2 samples of the second stage. The BS receives the pilot signal together with the interference reflected by the RIS, which is now employing the RIS phase-shift matrix $\mathbf{\Phi}^{(2)} \in \mathbb{C}^{\tau_2 \times N}$. The vector $\mathbf{y}_m^{(2)} \in \mathbb{C}^{\tau_2}$ received by antenna m at the BS is thus given by:

$$\mathbf{y}_m^{(2)} = \mathbf{\Phi}^{(2)}(\sqrt{\rho}\mathbf{g}_m \odot \mathbf{h} + \mathbf{g}_m \odot \mathbf{n}) + \mathbf{z}_m^{(2)}, \tag{9}$$

where $\mathbf{z}_m^{(2)} \sim \mathcal{N}_{\mathbb{C}}(\mathbf{0}_{\tau_2}, \sigma^2\mathbf{I}_{\tau_2})$ is additive Gaussian noise. Collecting all the vectors $\{\mathbf{y}_m^{(2)}; m = 1, \ldots, M\}$ into an $M\tau_2$-dimensional vector yields

$$\mathbf{y}^{(2)} = \sqrt{\rho}\mathbf{\Phi}_M^{(2)}\mathbf{x} + \mathbf{\Phi}_M^{(2)}\mathbf{e} + \mathbf{z}^{(2)}, \tag{10}$$

where $\mathbf{\Phi}_M^{(2)} = \mathbf{I}_M \otimes \mathbf{\Phi}^{(2)}$ and the NM-dimensional vector $\mathbf{x}$ is obtained by concatenating the vectors $\{\mathbf{g}_m \odot \mathbf{h}; m = 1, \ldots, M\}$. The covariance matrix of $\mathbf{x}$ is $\mathbf{R}_x = \mathbf{R}_{g'} \otimes (\mathbf{R}_g \odot \mathbf{R}_h)$ and its EVD is given by

$$\mathbf{R}_x = \mathbf{U}_x^{\text{s}} \mathbf{\Lambda}_x (\mathbf{U}_x^{\text{s}})^{\text{H}}. \tag{11}$$

The estimate $\hat{\mathbf{e}}_{\text{RS-LS}}$ in (7) is used to remove the interference from $\mathbf{y}^{(2)}$ to obtain

$$\bar{\mathbf{y}}^{(2)} = \mathbf{y}^{(2)} - \mathbf{\Phi}_M^{(2)} \hat{\mathbf{e}}_{\text{RS-LS}}. \tag{12}$$

The RS-LS estimate of $\mathbf{x}$ is thus computed as

$$\hat{\mathbf{x}}_{\text{RS-LS}} = \frac{1}{\sqrt{\rho}} \mathbf{U}_x^{\text{s}}\, \mathbf{F}\left(\mathbf{U}_x^{\text{s}}, \mathbf{\Phi}_M^{(2)}\right)^{-1} \mathbf{U}_x^{\text{s}\,\text{H}} \mathbf{\Phi}_M^{(2)\,\text{H}} \bar{\mathbf{y}}^{(2)}, \tag{13}$$

where $\mathbf{U}_x^{\text{s}}$ is the signal subspace of the correlation matrix $\mathbf{R}_x$. The MSE $\mathbb{E}\{||\hat{\mathbf{x}}_{\text{RS-LS}} - \mathbf{x}||^2\}$ takes the form:

$$\text{MSE}_x = \text{MSE}_x^{(1)} + \text{MSE}_x^{(2)}, \tag{14}$$

where $\mathrm{MSE}_x^{(1)}$ is given in (15), shown at the bottom of the page, and it is due to the interference estimation error, while the second term

$$\mathrm{MSE}_x^{(2)} = \frac{\sigma^2}{\rho}\,\mathrm{tr}\left\{\mathbf{F}\left(\mathbf{U}_x^{\mathrm{s}}, \mathbf{\Phi}_M^{(2)}\right)^{-1}\right\} \tag{16}$$

comes from the cascaded channel estimation error. We notice that (7) and (13) requires a priori information of the statistics of both interference and cascaded channels. In practice, this information may be difficult to obtain at the BS.

C. No a Priori Knowledge of Statistics

To dispense from knowledge of $\mathbf{R}_e$ and $\mathbf{R}_x$ (or $\mathbf{U}_e^{\mathrm{s}}$ and $\mathbf{U}_x^{\mathrm{s}}$), a possible solution is to utilize the subspace spanned by a known spatial correlation matrix $\overline{\mathbf{R}}$, which represents the union of the span of all plausible correlation matrices [9]. For this purpose, we use the following lemma proved in [11].

Lemma 1: Denote the two spatial correlation matrices obtained by the same array geometry as $\overline{\mathbf{R}}$ and $\mathbf{R}$, and the corresponding spatial scattering functions as $\bar{f}(\varphi,\theta)$ and $f(\varphi,\theta)$. Assume that $\bar{f}(\varphi,\theta)$ and $f(\varphi,\theta)$ are either continuous at each point on its domain or contain Dirac delta functions.

If the domain of $\bar{f}(\varphi,\theta)$ for which $\bar{f}(\varphi,\theta) > 0$ contains the domain of $f(\varphi,\theta)$ for which $f(\varphi,\theta) > 0$, and then the subspace spanned by the columns of $\overline{\mathbf{R}}$ would contain the subspace spanned by the columns of $\mathbf{R}$.

Since the spatial scattering functions for the isotropic case are non-zero for all the (φ,θ), the subspace spanned by the columns of correlation matrix $\overline{\mathbf{R}}_{\mathrm{iso}} = \overline{\mathbf{U}}_{\mathrm{iso}}^{\mathrm{s}}\mathbf{\Lambda}_{\mathrm{iso}}\overline{\mathbf{U}}_{\mathrm{iso}}^{\mathrm{s}\,\mathrm{H}}$ in (2) contains both the subspaces spanned by the columns of $\mathbf{R}_e$ and $\mathbf{R}_x$. Accordingly, assuming that $\bar{r} = \mathrm{rank}\{\overline{\mathbf{R}}_{\mathrm{iso}}\}$, an alternative representation of $\mathbf{e}$ and $\mathbf{x}$ is $\mathbf{e} = \overline{\mathbf{U}}_{\mathrm{iso}}^{\mathrm{s}}\mathbf{a}_{\mathrm{iso}}$ and $\mathbf{x} = \overline{\mathbf{U}}_{\mathrm{iso}}^{\mathrm{s}}\mathbf{b}_{\mathrm{iso}}$ with the reduced-dimension vectors $\{\mathbf{a}_{\mathrm{iso}}, \mathbf{b}_{\mathrm{iso}}\} \in \mathbb{C}^{\bar{r}}$, respectively. This yields the so-called *conservative RS-LS* estimate given by

$$\hat{\mathbf{e}}_{\mathrm{RS-LS}}^{\mathrm{con}} = \overline{\mathbf{U}}_{\mathrm{iso}}^{\mathrm{s}}\mathbf{F}\left(\overline{\mathbf{U}}_{\mathrm{iso}}^{\mathrm{s}}, \mathbf{\Phi}_M^{(1)}\right)^{-1}\overline{\mathbf{U}}_{\mathrm{iso}}^{\mathrm{s}\,\mathrm{H}}\mathbf{\Phi}_M^{(1)\mathrm{H}}\mathbf{y}^{(1)} \tag{17}$$

and

$$\hat{\mathbf{x}}_{\mathrm{RS-LS}}^{\mathrm{con}} = \frac{1}{\sqrt{\rho}}\overline{\mathbf{U}}_{\mathrm{iso}}^{\mathrm{s}}\mathbf{F}\left(\overline{\mathbf{U}}_{\mathrm{iso}}^{\mathrm{s}}, \mathbf{\Phi}_M^{(2)}\right)^{-1}\overline{\mathbf{U}}_{\mathrm{iso}}^{\mathrm{s}\,\mathrm{H}}\mathbf{\Phi}_M^{(2)\mathrm{H}}\bar{\mathbf{y}}^{(2)}. \tag{18}$$

In this case, the MSE expression simplifies to

$$\mathrm{MSE}_{\mathrm{iso},x} = \mathrm{MSE}_{\mathrm{iso},x}^{(1)} + \mathrm{MSE}_{\mathrm{iso},x}^{(2)} \tag{19}$$

with

$$\mathrm{MSE}_{\mathrm{iso},x}^{(i)} = \frac{\sigma^2}{\rho}\,\mathrm{tr}\left\{\mathbf{F}\left(\overline{\mathbf{U}}_{\mathrm{iso}}^{\mathrm{s}}, \mathbf{\Phi}_M^{(i)}\right)^{-1}\right\}. \tag{20}$$

IV. Optimal RIS Configuration for Estimation

To minimize $\mathrm{MSE}_{\mathrm{iso},x}$, we formulate the following optimization problem:

$$\min_{\tau_1,\tau_2,\mathbf{\Phi}^{(1)},\mathbf{\Phi}^{(2)}} \mathrm{MSE}_{\mathrm{iso},x},$$
$$\text{s.t. } \tau_1+\tau_2=\tau,\ |[\mathbf{\Phi}^{(i)}]_{j,n}| = 1,\ i\in\{1,2\}, \tag{21}$$

which is subject to the unit-modulus constraints of RIS elements. To obtain a closed-form solution, (21) is first relaxed as

$$\min_{\tau_1,\tau_2,\mathbf{\Phi}^{(1)},\mathbf{\Phi}^{(2)}} \mathrm{MSE}_{\mathrm{iso},x},$$
$$\text{s.t. } \tau_1+\tau_2=\tau,\ \mathrm{tr}\{\mathbf{\Phi}^{(i)\mathrm{H}}\mathbf{\Phi}^{(i)}\} \le N\tau_i,\ i\in\{1,2\}, \tag{22}$$

where the non-convex unit-modulus constraints are replaced by the Frobenius norm constraints on $\mathbf{\Phi}^{(i)}$. Then, considering the fact that $\overline{\mathbf{U}}_{\mathrm{iso}}^{\mathrm{s}} = \overline{\mathbf{U}}_{\mathrm{BS,s}}^{\mathrm{iso}} \otimes \overline{\mathbf{U}}_{\mathrm{RIS,s}}^{\mathrm{iso}}$ and $\mathbf{\Phi}_M^{(i)} = \mathbf{I}_M \otimes \mathbf{\Phi}^{(i)}$, the problem (22) can be further simplified as

$$\min_{\tau_1,\tau_2,\mathbf{\Phi}^{(1)},\mathbf{\Phi}^{(2)}} \frac{\sigma^2}{\rho} r_{\mathrm{BS}} \sum_{i=1,2}\mathrm{tr}\left\{\mathbf{F}\left(\overline{\mathbf{U}}_{\mathrm{RIS,s}}^{\mathrm{iso}}, \mathbf{\Phi}^{(i)}\right)^{-1}\right\},$$
$$\text{s.t. } \tau_1+\tau_2=\tau,\ \mathrm{tr}\{\mathbf{\Phi}^{(i)\mathrm{H}}\mathbf{\Phi}^{(i)}\} \le N\tau_i,\ i\in\{1,2\}, \tag{23}$$

where $r_{\mathrm{BS}} = \mathrm{rank}\{\overline{\mathbf{R}}_{\mathrm{BS}}^{\mathrm{iso}}\}$, $r_{\mathrm{RIS}} = \mathrm{rank}\{(\overline{\mathbf{R}}_{\mathrm{RIS}}^{\mathrm{iso}} \odot \overline{\mathbf{R}}_{\mathrm{RIS}}^{\mathrm{iso}})\}$, and $\overline{\mathbf{U}}_{\mathrm{BS,s}}^{\mathrm{iso}} \in \mathbb{C}^{M\times r_{\mathrm{BS}}}$ and $\overline{\mathbf{U}}_{\mathrm{RIS,s}}^{\mathrm{iso}} \in \mathbb{C}^{N\times r_{\mathrm{RIS}}}$ are the signal subspaces of $\overline{\mathbf{R}}_{\mathrm{BS}}^{\mathrm{iso}}$ and $(\overline{\mathbf{R}}_{\mathrm{RIS}}^{\mathrm{iso}} \odot \overline{\mathbf{R}}_{\mathrm{RIS}}^{\mathrm{iso}})$, respectively.

Let $\mathbf{A}_i \triangleq \mathbf{\Phi}^{(i)}\overline{\mathbf{U}}_{\mathrm{RIS,s}}^{\mathrm{iso}} \in \mathbb{C}^{\tau_i\times r_{\mathrm{RIS}}}, i\in\{1,2\}$. To accurately estimate the cascaded channel, it is necessary that $\mathbf{A}_i$ has full column rank, i.e., $\tau_i \ge r_{\mathrm{RIS}}\ \ (i=1,2)$, setting to $\tau = 2r_{\mathrm{RIS}}$ the minimum number of pilot time slots required in the training phase. Then, the optimization problem (23) can be reformulated as

$$\min_{\tau_1,\tau_2,\mathbf{\Phi}^{(1)},\mathbf{\Phi}^{(2)}} \frac{\sigma^2}{\rho} r_{\mathrm{BS}} \sum_{i=1,2}\sum_{p=1}^{r_{\mathrm{RIS}}}\frac{1}{\lambda_{A_i,p}^2},$$
$$\text{s.t. } \tau_i \ge r_{\mathrm{RIS}},\ \mathrm{tr}\{\mathbf{\Phi}^{(i)\mathrm{H}}\mathbf{\Phi}^{(i)}\} \le N\tau_i,\ i\in\{1,2\},$$
$$\tau_1+\tau_2=\tau, \tag{24}$$

where $\{\lambda_{A_i,p}\}$ is the set of non-zero singular values of $\mathbf{A}_i$. Considering that $\sum_p 1/\lambda_p^2$ is monotonically decreasing function of $\sum_p \lambda_p^2$, the minimization (24) can be recast as the maximization problem

$$\max_{\tau_1,\tau_2,\mathbf{\Phi}^{(1)},\mathbf{\Phi}^{(2)}} \frac{\sigma^2}{\rho} r_{\mathrm{BS}} \sum_{i=1,2}\mathrm{tr}\left\{\mathbf{F}\left(\overline{\mathbf{U}}_{\mathrm{RIS,s}}^{\mathrm{iso}}, \mathbf{\Phi}^{(i)}\right)\right\},$$
$$\text{s.t. } \tau_i \ge r_{\mathrm{RIS}},\ \mathrm{tr}\{\mathbf{\Phi}^{(i)\mathrm{H}}\mathbf{\Phi}^{(i)}\} \le N\tau_i,\ i\in\{1,2\},$$
$$\tau_1+\tau_2=\tau, \tag{25}$$

where

$$\mathrm{tr}\left\{\mathbf{F}\left(\overline{\mathbf{U}}_{\mathrm{RIS,s}}^{\mathrm{iso}}, \mathbf{\Phi}^{(i)}\right)\right\}$$
$$= \mathrm{tr}\left\{\mathbf{\Phi}^{(i)\mathrm{H}}\mathbf{\Phi}^{(i)}\right\} - \mathrm{tr}\left\{\mathbf{F}\left(\overline{\mathbf{U}}_{\mathrm{RIS,n}}^{\mathrm{iso}}, \mathbf{\Phi}^{(i)}\right)\right\} \le N\tau_i,$$

$i\in\{1,2\}$ and $\overline{\mathbf{U}}_{\mathrm{RIS,n}}^{\mathrm{iso}} \in \mathbb{C}^{N\times(N-r_{\mathrm{RIS}})}$ is the noise subspace of $\overline{\mathbf{R}}_{\mathrm{RIS}}^{\mathrm{iso}} \odot \overline{\mathbf{R}}_{\mathrm{RIS}}^{\mathrm{iso}}$. To solve (25), the right singular vectors of $\mathbf{\Phi}^{(i)}$ corresponding to the non-zero singular values should be orthogonal to $\overline{\mathbf{U}}_{\mathrm{RIS,n}}^{\mathrm{iso}}$, i.e., $\mathbf{\Phi}^{(i)}\overline{\mathbf{U}}_{\mathrm{RIS,n}}^{\mathrm{iso}} = \mathbf{0}$. Meanwhile, $\lambda_{A_i,p}$

$$\mathrm{MSE}_x^{(1)} = \frac{\sigma^2}{\rho}\,\mathrm{tr}\left\{\mathbf{F}\left(\mathbf{U}_x^{\mathrm{s}}, \mathbf{\Phi}_M^{(2)}\right)^{-2}\mathbf{U}_x^{\mathrm{s}\,\mathrm{H}}\mathbf{\Phi}_M^{(2)\mathrm{H}}\mathbf{\Phi}_M^{(2)}\mathbf{U}_e^{\mathrm{s}}\,\mathbf{F}\left(\mathbf{U}_e^{\mathrm{s}}, \mathbf{\Phi}_M^{(1)}\right)^{-1}\mathbf{U}_e^{\mathrm{s}\,\mathrm{H}}\mathbf{\Phi}_M^{(2)\mathrm{H}}\mathbf{\Phi}_M^{(2)}\mathbf{U}_x^{\mathrm{s}}\right\} \tag{15}$$

TABLE I
SIMULATION PARAMETERS

Case 1		Case 2		Case 3		Case 4	
Isotropic Channel & Isotropic Interference		Directional Channel & Isotropic Interference		Isotropic Channel & Directional Interference		Directional Channel & Directional Interference	
φ_h	$[-\frac{\pi}{2}, \frac{\pi}{2}]$	φ_h	70°	φ_h	$[-\frac{\pi}{2}, \frac{\pi}{2}]$	φ_h	70°
θ_h	$[-\frac{\pi}{2}, \frac{\pi}{2}]$	θ_h	-20°	θ_h	$[-\frac{\pi}{2}, \frac{\pi}{2}]$	θ_h	-20°
φ_g	$[-\frac{\pi}{2}, \frac{\pi}{2}]$	φ_g	-60°	φ_g	$[-\frac{\pi}{2}, \frac{\pi}{2}]$	φ_g	-60°
θ_g	$[-\frac{\pi}{2}, \frac{\pi}{2}]$	θ_g	-30°	θ_g	$[-\frac{\pi}{2}, \frac{\pi}{2}]$	θ_g	-30°
φ_n	$[-\frac{\pi}{2}, \frac{\pi}{2}]$	φ_n	$[-\frac{\pi}{2}, \frac{\pi}{2}]$	φ_n	-10°	φ_n	-10°
θ_n	$[-\frac{\pi}{2}, \frac{\pi}{2}]$	θ_n	$[-\frac{\pi}{2}, \frac{\pi}{2}]$	θ_n	20°	θ_n	20°
$\{f_i(\varphi_i, \theta_i) \vert i = g, h, n\}$: Gaussian Model							

$= \sqrt{N\tau_i / r_{\text{RIS}}}$ for $p = 1, 2, \ldots, r_{\text{RIS}}$, $i \in \{0, 1\}$. We thus design $\mathbf{\Phi}^{(i)}$ as follows:

$$\hat{\mathbf{\Phi}}^{(i)} = \sqrt{\frac{N\tau_i}{r_{\text{RIS}}}} \mathbf{V}_i \bar{\mathbf{U}}_{\text{RIS,s}}^{\text{iso}\,\text{H}}, \ i \in \{1, 2\}, \tag{26}$$

where $\mathbf{V}_i \in \mathbb{C}^{\tau_i \times r_{\text{RIS}}}$ is an arbitrary matrix with orthogonal columns. Plugging (26) into (23) and enforcing the constraint on the total number of pilot samples τ, the minimum MSE of the conservative RS-LS estimator is

$$\begin{aligned} \text{MSE}_{\text{iso},x}^{\min} &= \frac{\sigma^2}{\rho} \frac{r_{\text{BS}}}{N} \cdot r_{\text{RIS}}^2 \min_{\tau_1} \left(\frac{1}{\tau_1} + \frac{1}{\tau - \tau_1} \right) \\ &= \frac{\sigma^2}{\rho} \frac{r_{\text{BS}}}{N} \cdot \frac{4 r_{\text{RIS}}^2}{\tau}, \end{aligned} \tag{27}$$

which is obtained when $\tau_1 = \tau_2 = \tau/2$ and is inversely proportional to the numbers of RIS elements N and the total number of pilot samples. Furthermore, considering the unit-modulus constraints in (21), the optimal $\mathbf{\Phi}^{(i)}$ is ultimately constructed as

$$\mathbf{\Phi}_{\text{opt}}^{(i)} = e^{j \angle \hat{\mathbf{\Phi}}^{(i)}}, i \in \{1, 2\}. \tag{28}$$

V. NUMERICAL RESULTS

Numerical results are now given to assess the performance of the proposed channel estimation scheme. We assume the BS is equipped with $M = 16$ elements with $M_H = M_V = 4$, and the vertical and horizontal inter-antenna distances are set to $\lambda/4$, where λ is the wavelength. The RIS is equipped with $N = 256$ elements with $N_H = N_V = 16$, and the vertical and horizontal inter-element distances are set to $\lambda/8$. The ratio of the powers of signal and interference is set to $\rho/\sigma_n^2 = 12.5$ dB. The proposed scheme is tested studying the four different scenarios illustrated in Table I, where in case of directional channel or interference the angular spread is $\Delta = 20^\circ$.

The conservative RS-LS estimator is computed as in (28) and its results are indicated with the acronym 'con-RS-LS'. For the RS-LS scheme, whose MSE is calculated as in (14), the optimal RIS phase-shift matrix is practically impossible to obtain. Accordingly, we employ (26) and (28) to compute the phase-shift matrix $\mathbf{\Phi}^{(i)}$. As shown next, this heuristic choice of $\mathbf{\Phi}^{(i)}$ leads to good results, much better than those obtained with other more conventional choices such as, for example, employing the DFT matrix of size N. It is essential to emphasize that the results obtained using the RS-LS method represent the ideal scenario where the actual correlation matrices, $\mathbf{R}_e$ and $\mathbf{R}_x$, are known. Even in cases where these matrices are unknown, the RS-LS results provide an estimate of the approximate performance degradation caused by using an isotropic correlation matrix.

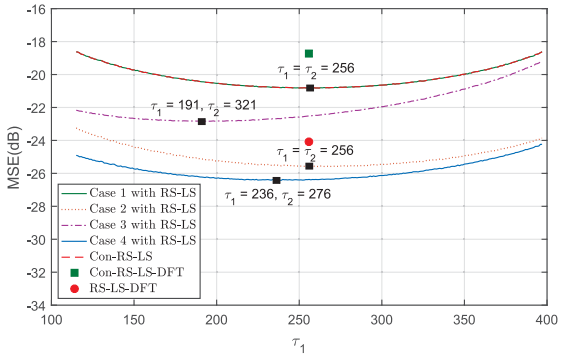

Fig. 1. The MSEs vs. τ_1 with different estimators in different channel and interference scenarios at SNR =15dB.

Fig. 1 reports the MSE as a function of the pilot length τ_1, when $\tau = \tau_1 + \tau_2 = 2N = 512$ and $\text{SNR} = \rho/\sigma^2 = 15$ dB. In case 1, where everything is isotropic, the performance of the two schemes are identical and the optimal pilot allocation is $\tau_1 = \tau_2$. The RS-LS estimator, leveraging improved knowledge of channel statistics, consistently outperforms the conventional RS-LS estimator in all other scenarios. The optimal value of τ_1 varies depending on the specific case. Furthermore, while the performance of the conventional RS-LS scheme remains unaffected by the statistical characteristics of the channel, the RS-LS estimator exhibits lower MSE in the presence of a directional channel (cases 2 and 4) compared to an isotropic channel. As a point of reference, the figure also displays the results obtained for the conventional RS-LS scheme when the RIS phase-shift matrix is the DFT matrix of size N. The remaining simulations will investigate the algorithm's performance specifically for the challenging channel configuration of Case 4.

Fig. 2 plots the MSE as a function of the SNR in dB when $\tau_1 = \tau_2 = N$: the suffix '-DFT' indicates the case when the RIS phase-shifts matrix is the DFT matrix, the suffix '-bound' is the bound obtained employing the RIS phase-shifts matrix in (26). Table II reports the MSEs of various estimators at an SNR of 10 dB, enabling a straightforward performance comparison. The impact of interference cancellation is first evaluated. When interference is not canceled, both estimation schemes quickly reach a floor of irreducible MSE, highlighting the need to address the interference problem. Among the schemes performing interference cancellation, the best results are obtained by the RS-LS estimator, with a MSE

TABLE II
THE MSE (DB) UNDER SNR=10DB

	RS-LS-DFT	RS-LS	RS-LS-random	RS-LS w/o Int. est	con-RS-LS-DFT	con-RS-LS-bound	con-RS-LS	con-RS-LS-random	con-RS-LS w/o Int. est
$\tau_1 = \tau_2 = N$	-14.09	-16.39	-	14.12	-8.70	-12.18	-10.81	-	14.15
$\tau_1 = \tau_2 = r_{\text{RIS}} + 1$	-	-12.53	0.87	-	-	-8.74	-6.57	19.78	-

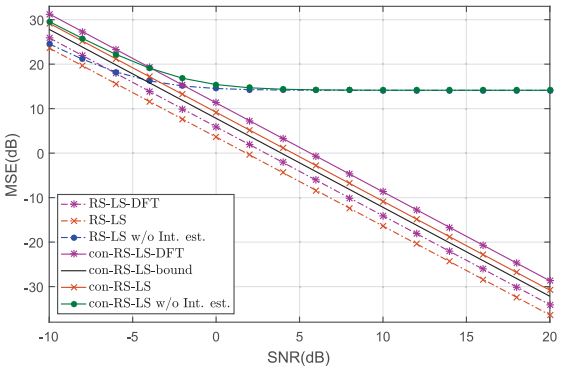

Fig. 2. The MSEs vs. SNR for different estimators and RIS phase-shift configurations with $\tau_1 = \tau_2 = N$.

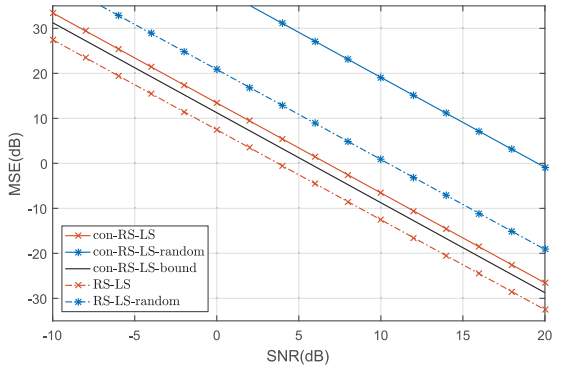

Fig. 3. MSEs vs. SNR for different estimators with different RIS phase-shift configurations and $\tau_1 = \tau_2 = r_{\text{RIS}} + 1$.

improvement of over 30 dB compared to no interference cancellation. Utilizing the phase-shifts matrix (28) yields a gain of 2.3 dB over RS-LS-DFT, indicating that optimized RIS phase-shifts in the isotropic case can seamlessly enhance the performance of the RS-LS estimator. When lacking a priori knowledge of the channel and interference statistics, the con-RS-LS estimator yields the best results, closely approaching the bound that does not consider the unit modulus constraint for RIS coefficients. Conversely, the con-RS-LS-DFT estimator performs the worst, with an approximate 2 dB MSE loss compared to the former estimator.

One of the key advantages of both the RS-LS and con-RS-LS estimators is their ability to reduce the required number of pilots compared to the conventional approach of employing a square $N \times N$ RIS phase-shift matrix. The objective function in (23) reveals that the minimum number of pilots required is $2r_{\text{RIS}}$. This reduction in pilot overhead is a significant benefit of these estimators. Fig. 3 plots the RS-LS and con-RS-LS results when the number of pilots time is $\tau_1 = \tau_2 = r_{\text{RIS}} + 1$, where $r_{\text{RIS}} = 115$ is the effective rank of $\overline{\mathbf{R}}_{\text{RIS}}^{\text{iso}} \odot \overline{\mathbf{R}}_{\text{RIS}}^{\text{iso}}$ containing a fraction $1-10^{-4}$ of the sum of all eigenvalues. In this particular configuration, the estimators utilizing DFT phase-shifts are not applicable. Therefore, we consider estimators with random unit-modulus RIS phase-shifts as an alternative benchmark. The results in Table II clearly demonstrate the significant gaps of over 10 dB and 20 dB between the random and optimized phase-shifts for the RS-LS and conservative RS-LS algorithms, respectively. This highlights the effectiveness of the proposed channel estimation scheme, even when the total number of pilot time slots is less than N.

VI. CONCLUSION

In this letter, we presented a channel estimation scheme specifically designed for wireless communications assisted by RIS in the presence of interference. The proposed solution consists of two phases: interference estimation and removal in the first phase, followed by cascaded channel estimation in the second phase. Importantly, the scheme does not rely on any prior knowledge of the spatial correlation matrices of the interference or cascaded channel. Furthermore, we optimized the phase-shifts of the RIS to ensure accurate channel estimation with reduced pilot overhead. Numerical results demonstrated the effectiveness of the proposed scheme compared to existing alternatives that overlook the presence of interference.

REFERENCES

[1] M. Di Renzo et al., "Smart radio environments empowered by reconfigurable intelligent surfaces: How it works, state of research, and the road ahead," *IEEE J. Sel. Areas Commun.*, vol. 38, no. 11, pp. 2450–2525, Nov. 2020.

[2] W. Long, R. Chen, M. Moretti, W. Zhang, and J. Li, "A promising technology for 6g wireless networks: Intelligent reflecting surface," *J. Commun. Inf. Netw.*, vol. 6, no. 1, pp. 1–16, Mar. 2021.

[3] E. Björnson, H. Wymeersch, B. Matthiesen, P. Popovski, L. Sanguinetti, and E. de Carvalho, "Reconfigurable intelligent surfaces: A signal processing perspective with wireless applications," *IEEE Signal Process. Mag.*, vol. 39, no. 2, pp. 135–158, Mar. 2022.

[4] A. de Jesus Torres, L. Sanguinetti, and E. Björnson, "Electromagnetic interference in RIS-aided communications," *IEEE Wireless Commun. Lett.*, vol. 11, no. 4, pp. 668–672, Apr. 2022.

[5] A. Khaleel and E. Basar. "Electromagnetic interference cancellation for RIS-assisted communications." Apr. 2023. [Online]. Available: https://arxiv.org/abs/2304.04476.

[6] E. Shtaiwi, H. Zhang, S. Vishwanath, M. Youssef, A. Abdelhadi, and Z. Han, "Channel estimation approach for RIS assisted MIMO systems," *IEEE Trans. Cogn. Commun. Netw.*, vol. 7, no. 2, pp. 452–465, Jun. 2021.

[7] B. Zheng, C. You, W. Mei, and R. Zhang, "A survey on channel estimation and practical passive beamforming design for intelligent reflecting surface aided wireless communications," *IEEE Commun. Surveys Tuts.*, vol. 24, no. 2, pp. 1035–1071, 2nd Quart., 2022.

[8] G. Zhou, C. Pan, H. Ren, P. Popovski, and A. L. Swindlehurst, "Channel estimation for RIS-aided multiuser millimeter-wave systems," *IEEE Trans. Signal Process.*, vol. 70, pp. 1478–1492, Mar. 2022.

[9] Ö. T. Demir, E. Björnson, and L. Sanguinetti, "Exploiting array geometry for reduced-subspace channel estimation in RIS-aided communications," in *Proc. IEEE 12th Sensor Array Multichannel Signal Process. Workshop (SAM)*, 2022, pp. 455–459.

[10] E. Björnson and L. Sanguinetti, "Rayleigh fading modeling and channel hardening for reconfigurable intelligent surfaces," *IEEE Wireless Commun. Lett.*, vol. 10, no. 4, pp. 830–834, Apr. 2021.

[11] Ö. T. Demir, E. Björnson, and L. Sanguinetti, "Channel modeling and channel estimation for holographic massive MIMO with planar arrays," *IEEE Wireless Commun. Lett.*, vol. 11, no. 5, pp. 997–1001, May 2022.